



INAOE

Time-bandwidth product of the acousto-optical cells

Principle contributors:

**Alexandre S. Shcherbakov⁽¹⁾,
Ana Virginia Hanessian de la Garza⁽¹⁾,
Sergey A. Nemov⁽²⁾, and Daniel Sanchez Lucero⁽¹⁾.**

1) National Institute for Astrophysics, Optics, and Electronics
(INAOE), Puebla, 72000, Mexico.

2) Saint – Petersburg State Polytechnic University, St-Petersburg,
195251, Russian Federation

**National Institute for Astrophysics, Optics,
and Electronics (INAOE)**

Puebla, Mexico.

Department for Optics, INAOE

INAOE, 2012

The authors hereby grant to INAOE
permission to reproduce and distribute
copies of this technical report.



INDEX

Abstract	3
1. Introduction	3
2. Efficiency of a few selected crystalline acousto-optical materials operating in Bragg regime of the normal light scattering	4
2.1. The Bragg regime of the normal light scattering in an acousto-optical cell.....	4
2.2. Efficiency of light scattering in a lead molybdate single crystal.....	5
2.3. Efficiency of light scattering in a tellurium dioxide crystal exited by the longitudinal acoustic mode passing along the [001]-axis.....	7
2.4. Efficiency of light scattering in a gallium phosphide single crystal.....	9
2.5. Linear attenuation of the longitudinal elastic waves and its effect on the efficiency of light scattering.....	11
3. Estimating the time – bandwidth product of acousto-optical cells operating in the normal light scattering regime in some crystals	15
3.1. Time-bandwidth product of the acousto-optical cells based on a lead molybdate (PbMoO_4) single crystal.....	16
3.2. Time-bandwidth product of the acousto-optical cells using a tellurium dioxide crystal (TeO_2) single crystal exited by the longitudinal acoustic mode passing along the [001]-axis.....	17
3.3. Time-bandwidth product of the acousto-optical cells based on gallium phosphide (GaP) single crystal.....	18
4. Time-bandwidth product of the acousto-optical cells based on the non-degenerated anomalous light scattering in TeO_2 crystal	19
4.1. Non-degenerated anomalous Bragg light scattering in a crystalline material.....	19
4.2. Estimating the time – bandwidth product of acousto-optical cell operating in the non-degenerated anomalous light scattering regime.....	20
4.3. Experimental data.....	22
5. Conclusive remarks	25
6. Acknowledgement	25
7. References	25

Abstract

Basic performances of the acousto-optical cells, which can be potentially involved into creating the frontier acousto-optical systems for data processing such as the advanced spectrometers for the spectrum analysis of both optical and radio-wave signals with radically improved resolution or a novel triple-product acousto-optical processor for modern astrophysical applications, are under consideration. During the presented analysis we restrict ourselves by the Bragg limit of light scattering into the first order. The attention is paid at first to determining the expected efficiency of a few acousto-optical crystalline materials and then mainly to estimating the time-bandwidth product of acousto-optical cells, because just the last parameter can be taken as the most general one for the characterization of performance data inherent in each individual cell. Functional capabilities peculiar to the cells operating over either normal or anomalous light scattering regime are under discussion. Evidently, the anomalous regime of light scattering promises better results. Both the theoretical estimations and the experimental data obtained for a large-aperture acousto-optical cell based on a tellurium dioxide crystal, exploiting the non-degenerated anomalous light scattering, gives rather high the time-bandwidth product equal to about **4000** .

Key words: spectrum analysis, acousto-optical cell, time-bandwidth product, crystalline material.

1. Introduction

Performance data of any optical system for a high-bit-rate data processing based on acousto-optical technique are mainly determined by parameters of each particular acousto-optical cell (AOC) exploited within the chosen schematic arrangement. Here, certain of basic properties peculiar to the AOCs, involved into creating the frontier acousto-optical systems for data processing such as the advanced spectrometers for the spectrum analysis of both optical and radio-wave signals with radically improved resolution or a novel triple-product acousto-optical processor for modern astrophysical applications, are under consideration. Because practical applications of these processors are oriented to investigations in extra-galactic astronomy as well as of extra-solar planets, the algorithm of so-called space-and-time integrating will be realized to provide spectrum analysis of rather low-power signals in a wide frequency bandwidth with an improved spectral resolution. These circumstances dictate us updated requirements to the AOCs due to be applied in the status of deflectors as one-dimensional input devices for a two-dimensional optical processing. Generally, information capabilities of the AOCs are determined by the time-bandwidth product (TBWP), which is defined as the product of the device time aperture and the frequency bandwidth inherent in a cell. Formally, the TBWP is equivalent to the number of resolvable spots, defined in its turn as the ratio of maximum deflection angle over the angular divergence of the diffraction-limited optical beam. In acousto-optical deflectors, the TBWP determines the frequency resolution (when they used in the space-integrating spectrum analyzers) or the processing gain (in the space-integrating correlators), or the number of parallel correlations (in the time-integrating correlators). Rather accurate estimations for deflectors can be obtained using the procedure developed in Ref.[1.1], which takes into account a triplet of key factors: (a) available optical aperture, (b) the acoustic beam divergence conditioned by the piezoelectric transducer length, and (c) acceptable level of acoustic beam attenuation along optical aperture. Here, just this procedure is mainly exploited, but it should be noted that similar approach excludes such really important factors as the level of acoustic power density applied to various AOCs and the available light diffraction efficiency per each individual resolvable spot. In fact, these two factors are related to the problem of exhibiting potential acoustic and acousto-optical nonlinearities within signal processing system. However, in our particular case of astrophysical applications one can expect relatively low levels of the input signals, so that, for instance, the diffraction efficiency will definitely not exceed **1%** .

2. Efficiency of a few selected crystalline acousto-optical materials operating in Bragg regime of the Normal light scattering

2.1. THE BRAGG REGIME OF THE NORMAL LIGHT SCATTERING IN AN ACOUSTO-OPTICAL CELL

One of the limiting regimes of light diffraction occurs with a large length L and at rather high frequency of the acoustic wave injected into a medium. In this case, the dynamic acoustic grating is rather thick, so that during the analysis of diffraction one has to take account of the phase relations between waves in different orders. Such a regime can be realized only when the angle of light incidence θ_B on a thick dynamic acoustic grating meets the Bragg condition $\sin \theta_B = \lambda/2n\Lambda$ and inequality $Q = 2\pi\lambda L/\Lambda^2 \gg 1$ [2.1]. Usually, the Bragg regime includes the incident and just one scattered light modes as well as the acoustic mode, see Fig.2.1a, and during the presented analysis we restrict ourselves by the Bragg limit of light scattering into the first order. Moreover, the normal process of light scattering implies that the initial state of light polarization will not be changed within the process of interaction between optical and acoustical beams in spite of exploiting various crystalline materials in the acousto-optical cells under consideration.

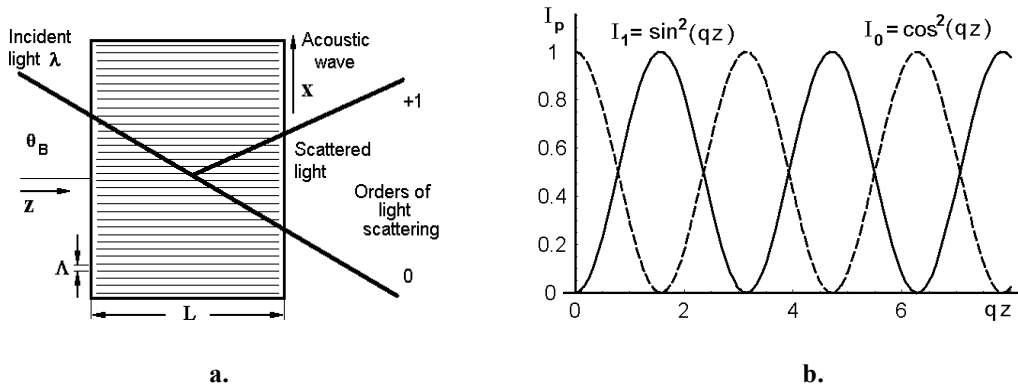


Figure 2.1. Scattering light by a thick dynamic acoustic gratings (a) and the light intensities in various orders of light scattering in the Bragg limit (b).

The light intensities in two orders of scattering are shown in Fig.2.1b, where $q = \pi (\lambda \cos \theta_B)^{-1} \sqrt{M_2 P / 2}$ [2.2], M_2 is the acousto-optic figure of merit, P is the acoustic power density. This figure illustrates just the Bragg limits of light diffraction. One can see that the Bragg regime is preferable for practical applications due to an opportunity to realize a **100%** efficiency of light scattering by the coherent acoustic phonons.

The conservation laws inherent in such interactions are $\vec{k}_1 + \vec{k}_2 = \vec{k}_3$ for the wave vectors (or the momenta $\vec{p} = \hbar \vec{k}$) and $\omega_1 + \omega_2 = \omega_3$ for the angular frequencies (or the energies $E = \hbar \omega$). Usually within conventional acousto-optics, $\omega_1, \omega_3 \cong 10^{14}$ Hz and $\omega_2 = \Omega \leq 10^9$ Hz, so that $\Omega/\omega_1 \approx 10^{-5}$ and $E_{\text{photon}} \approx 10^5 E_{\text{phonon}}$. Because $c = 3 \cdot 10^{10}$ cm/s and $V \approx 3 \cdot 10^5$ cm/s, we yield $V/c \approx 10^{-5}$, $\omega_1/c \approx \Omega/V$, and $k_{\text{photon}} \approx K_{\text{phonon}}$. Thus, if the powers of light and ultrasound have the same order, one has much more (about 10^5) phonons than photons in such an experiment. By this is meant that the acousto-optical interaction can be considered in an approximation of a given acoustic wave field.

2.2. EFFICIENCY OF LIGHT SCATTERING IN A LEAD MOLYBDATE CRYSTAL

The acousto-optic figure of merit M_2 describes the material properties relative to normal process of light scattering. It is given by [2.3]

$$M_2 = \frac{p_{\text{eff}}^2 n^6}{\rho V^3}, \quad (2.1)$$

where n is the corresponding refractive index, $\rho = 6.95 \text{ g/cm}^3$ is the material density of a lead molybdate crystal (PbMoO_4), and p_{eff} is the corresponding effective photo-elastic constant. The main values N_E and N_O of the refractive indices inherent in a lead molybdate crystal are slightly dispersive, i.e.: $N_E = 2.262$, $N_O = 2.386$ at $\lambda = 632.8 \text{ nm}$; $N_E = 2.2814$, $N_O = 2.381$ at $\lambda = 546 \text{ nm}$; $N_E = 2.315$, $N_O = 2.469$ at $\lambda = 514.5 \text{ nm}$; $N_E = 2.335$, $N_O = 2.502$ at $\lambda = 488 \text{ nm}$; $N_E = 2.528$, $N_O = 2.349$ at $\lambda = 471.3 \text{ nm}$; $N_E = 2.576$, $N_O = 2.375$ at $\lambda = 447.1 \text{ nm}$; and $N_E = 2.443$, $N_O = 2.719$ at $\lambda = 404.6 \text{ nm}$. Now, however, the main attention should be paid to determining concrete magnitudes of both p_{eff} and M_2 . In so doing, one has to consider the photo-elastic properties of lead molybdate single crystal. Generally, the dielectric impermeability tensor $\hat{\kappa}$ becomes to be perturbed under action of mechanical deformations in a medium and takes the form $\hat{\kappa} + \hat{\zeta}$, where the symmetrical tensor $\hat{\zeta}$ of the second rank presents small admixture to the tensor $\hat{\kappa}$. In so doing, one can write $\hat{\zeta} = \hat{\mathbf{p}}\hat{\gamma}$ or the same in components $\zeta_{ij} = \mathbf{p}_{ijkl} \gamma_{kl}$, because even the first approximation is quite enough for crystalline materials. Here, $\hat{\mathbf{p}}$ is the tensor of the fourth rank for photo-elastic coefficients; its symmetry is $\mathbf{p}_{ijkl} = \mathbf{p}_{jikl} = \mathbf{p}_{ijlk} = \mathbf{p}_{jilk}$, that is why the photo-elastic effect can be observed in media of an arbitrary symmetry, even in isotropic ones. Mechanical deformations are described in the same first approximation by the symmetric deformation tensor

$$\text{a) } \gamma_{kl} = \frac{1}{2\mathbf{K}} \left(\frac{\partial \bar{\mathbf{u}}_k}{\partial x_l} + \frac{\partial \bar{\mathbf{u}}_l}{\partial x_k} \right), \quad \text{b) } \gamma_{kl} = \gamma_{lk}, \quad (2.2)$$

where $\bar{\mathbf{u}}$ is the unit vector of displacement in the acoustic wave. Due to $\partial \bar{\mathbf{u}}(\bar{\mathbf{r}}, \mathbf{t}) / \partial \bar{\mathbf{r}} = i\bar{\mathbf{K}} \cdot \bar{\mathbf{u}}$ for the monochromatic plane acoustic wave with the wave vector $\bar{\mathbf{K}} = \mathbf{K}\bar{\mathbf{m}}$, we yield $\hat{\gamma} = \frac{1}{2}(\bar{\mathbf{u}} \cdot \bar{\mathbf{m}} + \bar{\mathbf{m}} \cdot \bar{\mathbf{u}})$. Practically, it is more convenient to operate by these tensors in matrix notations [2.4] (with the Greek letter indices) when $\zeta_\lambda = \zeta_{ij}$ with $(ij \leftrightarrow \lambda = 1, 2, \dots, 6)$, $\mathbf{p}_{\lambda\mu} = \mathbf{p}_{ijkl}$ with $(ij \leftrightarrow \lambda = 1, 2, \dots, 6; \mathbf{kl} \leftrightarrow \mu = 1, 2, \dots, 6)$, $\gamma_\mu = \gamma_{kl}$ with $(\mathbf{kl} \leftrightarrow \mu = 1, 2, 3)$, and $\gamma_\mu = 2\gamma_{kl}$ with $(\mathbf{kl} \leftrightarrow \mu = 4, 5, 6)$, so that $\zeta_\lambda = \mathbf{p}_{\lambda\mu} \gamma_\mu$. The quadratic form

$$\text{a) } \mathbf{p}_{\text{eff}} = \bar{\mathbf{d}}^{(s)} \cdot \hat{\zeta} \cdot \bar{\mathbf{d}}^{(i)}, \quad \text{b) } \mathbf{p}_{\text{eff}} = \mathbf{d}_i^{(s)} \zeta_{ij} \mathbf{d}_j^{(i)} \quad (2.3)$$

describes the effective photo-elastic constant \mathbf{p}_{eff} of the scattering process, i.e. the efficiency of converting the initial state of light polarization, described by the unit vector $\bar{\mathbf{d}}^{(i)}$ oriented along the corresponding electric induction vector $\bar{\mathbf{D}}^{(i)}$ into the scattered state of light polarization, characterized by the unit vector

$\bar{\mathbf{d}}^{(s)}$ oriented along the corresponding electric induction vector $\bar{\mathbf{D}}^{(s)}$ due to the photo-elastic effect (or what is the same, the acousto-optical interaction) in a crystal. In the case of a **PbMoO₄**-crystal, whose point symmetry group is 4/m, one can write [2.4]

$$\mathbf{p}_{\lambda\mu} = \begin{pmatrix} \mathbf{p}_{11} & \mathbf{p}_{12} & \mathbf{p}_{13} & \mathbf{0} & \mathbf{0} & \mathbf{p}_{16} \\ \mathbf{p}_{12} & \mathbf{p}_{11} & \mathbf{p}_{13} & \mathbf{0} & \mathbf{0} & -\mathbf{p}_{16} \\ \mathbf{p}_{31} & \mathbf{p}_{31} & \mathbf{p}_{33} & \mathbf{0} & \mathbf{0} & \mathbf{0} \\ \mathbf{0} & \mathbf{0} & \mathbf{0} & \mathbf{p}_{44} & \mathbf{p}_{45} & \mathbf{0} \\ \mathbf{0} & \mathbf{0} & \mathbf{0} & -\mathbf{p}_{45} & \mathbf{p}_{44} & \mathbf{0} \\ \mathbf{p}_{61} & -\mathbf{p}_{61} & \mathbf{0} & \mathbf{0} & \mathbf{0} & \mathbf{p}_{66} \end{pmatrix} \quad (2.4)$$

in the standard crystallographic axes. Then, let us assume that slow longitudinal acoustic wave is passing along the **[001]**-axis in a **PbMoO₄** -crystal whose vector of displacement is oriented along the same **[001]**-axis. By this it means that $\bar{\mathbf{m}} = \bar{\mathbf{u}} = (\mathbf{0}, \mathbf{0}, \mathbf{1}) = \bar{\mathbf{e}}_3$. The corresponding normalized tensor of deformations is given by $\hat{\gamma} = \bar{\mathbf{e}}_3 \cdot \bar{\mathbf{e}}_3$ or in matrix notations by $\gamma_{\mu} = (\mathbf{0}, \mathbf{0}, \mathbf{1}, \mathbf{0}, \mathbf{0}, \mathbf{0})$. Performing the matrix multiplication and converting the product $\mathbf{p}_{\lambda\mu} \gamma_{\mu}$ to the conventional indices, one can obtain the admixtures ζ_{ij} to the dielectric impermeability tensor $\hat{\mathbf{k}}$ in the form

$$\hat{\zeta} = \hat{\mathbf{p}} \hat{\gamma} = \mathbf{p}_{13} (\bar{\mathbf{e}}_1 \cdot \bar{\mathbf{e}}_1 + \bar{\mathbf{e}}_2 \cdot \bar{\mathbf{e}}_2) + \mathbf{p}_{33} (\bar{\mathbf{e}}_3 \cdot \bar{\mathbf{e}}_3). \quad (2.5)$$

The matrix of admixtures $\hat{\zeta}$ is a diagonal one, so that only normal light scattering will have place, i.e. $\bar{\mathbf{d}}^{(s)} = \bar{\mathbf{d}}^{(i)} = \bar{\mathbf{d}}$. Using Eqs.(2.3) and (2.5), the effective photo-elastic constant can be written as

$$\mathbf{p}_{\text{eff}} = \bar{\mathbf{d}} \hat{\zeta} \bar{\mathbf{d}} = \bar{\mathbf{d}} \begin{pmatrix} \mathbf{p}_{13} & \mathbf{0} & \mathbf{0} \\ \mathbf{0} & \mathbf{p}_{13} & \mathbf{0} \\ \mathbf{0} & \mathbf{0} & \mathbf{p}_{33} \end{pmatrix} \bar{\mathbf{d}}. \quad (2.6)$$

Due to $\bar{\mathbf{K}} \parallel [\mathbf{001}]$, it is obvious that if the Bragg angles are omitted as small values, the wave vectors $\bar{\mathbf{k}}_0$ and $\bar{\mathbf{k}}_1$ of the incident and scattered light beams, respectively, should lie in the **(001)**-plane to be orthogonal to $\bar{\mathbf{K}}$. Moreover, one can put $\bar{\mathbf{k}}_0 = \bar{\mathbf{k}}_1 = \bar{\mathbf{k}}$ when the Bragg angles are neglected, so that one may write $\bar{\mathbf{k}}_{0,1} \equiv \bar{\mathbf{k}} = (\cos \alpha, \sin \alpha, \mathbf{0})$, where the angle α as current angle between $\bar{\mathbf{k}}$ and $\bar{\mathbf{e}}_1 \parallel [\mathbf{100}]$. The vector $\bar{\mathbf{k}}$ and axis **[001]** give us an orthogonal basis to explain the vector $\bar{\mathbf{d}}$. Consequently, one can easily obtain that $\bar{\mathbf{d}} = (-\sin \alpha \cdot \sin \beta, \cos \alpha \cdot \sin \beta, \cos \beta)$, so that $\bar{\mathbf{d}} \parallel [\mathbf{001}]$ when $\beta = \mathbf{0}$. As a result, one yields

$$\mathbf{p}_{\text{eff}} = \mathbf{p}_{13} \sin^2 \beta + \mathbf{p}_{33} \cos^2 \beta. \quad (2.7)$$

This formula was simulated numerically with $\mathbf{p}_{13} = \mathbf{0.255}$ and $\mathbf{p}_{33} = \mathbf{0.300}$, see Ref.[2.5, 2.6]; the plot is shown in Fig.2.2. The availability of maxima for \mathbf{M}_2 depends radically on the magnitude of the refractive index as well.

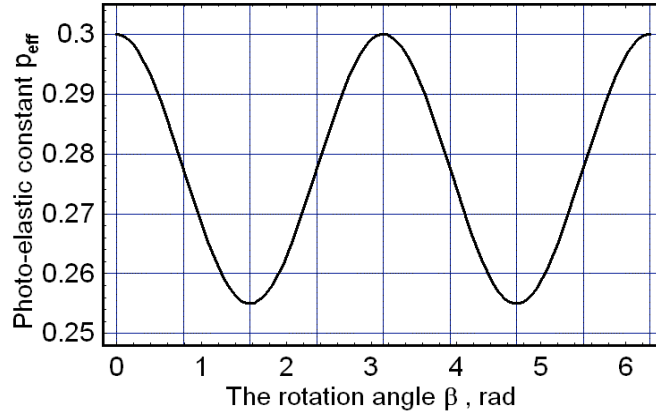


Figure 2.2. Dependence for the effective photo-elastic constant in a **PbMoO₄** single crystal versus the rotation angle β inherent in the normal light scattering.

Due to $\vec{k} \parallel [001]$ in a uniaxial crystal, the eigen-states of light polarization are naturally associated with the refractive indices N_O when $\beta = \pi k$ and N_E when $\beta = (\pi/2) + \pi k$. Because $N_O < N_E$ in a **PbMoO₄** single crystal, the problem needs additional estimations of maxima for M_2 . At the light wavelength $\lambda = 633$ nm, for example, this crystal has $N_E = 2.386$ and $N_O = 2.262$, so that, using the above-obtained data for p_{eff} , one can find $M_2 = 36.3 \cdot 10^{-18} \text{ s}^3/\text{g}$ for $\beta = \pi k$ and $M_2 = 36.1 \cdot 10^{-18} \text{ s}^3/\text{g}$ for $\beta = (\pi/2) + \pi k$. The performed calculations demonstrate that the normal regime of light scattering by the longitudinal elastic wave is rather efficient in the chosen crystal.

2.3. EFFICIENCY OF LIGHT SCATTERING IN A TELLURIUM DIOXIDE CRYSTAL EXCITED BY THE LONGITUDINAL ACOUSTIC MODE PASSING ALONG THE [001]-AXIS

Characterizing the efficiency of light scattering by acoustic waves is connected again with estimating the factor q , which describes both the material properties relative to the process and the acoustic power density. Generally, main values N_E and N_O of the refractive indices in optically anisotropic tellurium dioxide crystal are, for example, $N_E = 2.41$, $N_O = 2.26$ at $\lambda = 633$ nm and $N_E = 2.49$, $N_O = 2.33$ at $\lambda = 488$ nm. Now, however, the main attention should be paid to determining concrete magnitudes of the needed effective photo-elastic constant p_{eff} and the figure of acousto-optical merit M_2 in a **TeO₂**-based crystalline cell. In so doing, one has to consider the photo-elastic properties of this crystal using the approach described previously. In the case of a **TeO₂**-crystal, whose point symmetry group is 422, one can write [2.4] that

$$p_{\lambda\mu} = \begin{pmatrix} p_{11} & p_{12} & p_{13} & 0 & 0 & 0 \\ p_{12} & p_{11} & p_{13} & 0 & 0 & 0 \\ p_{31} & p_{31} & p_{33} & 0 & 0 & 0 \\ 0 & 0 & 0 & p_{44} & 0 & 0 \\ 0 & 0 & 0 & 0 & p_{44} & 0 \\ 0 & 0 & 0 & 0 & 0 & p_{66} \end{pmatrix} \quad (2.8)$$

in the standard crystallographic axes. Then, let us assume that the longitudinal acoustic wave is passing along the $[001]$ -axis in a TeO_2 -crystal whose vector of displacement is oriented along the same $[001]$ -axis. By this it means that $\bar{\mathbf{m}} = \bar{\mathbf{u}} = (0, 0, 1) = \bar{\mathbf{e}}_3$. The corresponding normalized tensor of deformations is given by $\hat{\gamma} = \bar{\mathbf{e}}_3 \cdot \bar{\mathbf{e}}_3$ or in matrix notations by $\gamma_\mu = (0, 0, 1, 0, 0, 0)$. Performing the matrix multiplication and converting the product $\mathbf{p}_{\lambda\mu} \gamma_\mu$ to the conventional indices, one can obtain the admixtures ζ_{ij} to the dielectric impermeability tensor $\hat{\kappa}$ in the form

$$\hat{\zeta} = \hat{\mathbf{p}} \hat{\gamma} = \mathbf{p}_{13} (\bar{\mathbf{e}}_1 \cdot \bar{\mathbf{e}}_1 + \bar{\mathbf{e}}_2 \cdot \bar{\mathbf{e}}_2) + \mathbf{p}_{33} (\bar{\mathbf{e}}_3 \cdot \bar{\mathbf{e}}_3). \quad (2.9)$$

The matrix of admixtures $\hat{\zeta}$ is a diagonal one, so that only normal light scattering will have place, i.e.

$\bar{\mathbf{d}}^{(s)} = \bar{\mathbf{d}}^{(i)} = \bar{\mathbf{d}}$. Using the conventional formula $\mathbf{p}_{\text{eff}} = \bar{\mathbf{d}}^{(s)} \cdot \hat{\zeta} \cdot \bar{\mathbf{d}}^{(i)}$ and Eq.(2.9), the effective photo-elastic constant can be written as

$$\mathbf{p}_{\text{eff}} = \bar{\mathbf{d}} \hat{\zeta} \bar{\mathbf{d}} = \bar{\mathbf{d}} [\mathbf{p}_{13} (\bar{\mathbf{e}}_1 \cdot \bar{\mathbf{e}}_1 + \bar{\mathbf{e}}_2 \cdot \bar{\mathbf{e}}_2) + \mathbf{p}_{33} (\bar{\mathbf{e}}_3 \cdot \bar{\mathbf{e}}_3)] \bar{\mathbf{d}}. \quad (2.10)$$

Due to $\bar{\mathbf{K}} \parallel [001]$, it is obvious that if the Bragg angles are omitted as small values, the wave vectors $\bar{\mathbf{k}}_0$ and $\bar{\mathbf{k}}_1$ of the incident and scattered light beams, respectively, should lie in the (001) -plane to be orthogonal to $\bar{\mathbf{K}}$. Moreover, one can put $\bar{\mathbf{k}}_0 = \bar{\mathbf{k}}_1 = \bar{\mathbf{k}}$ when the Bragg angles are neglected, so that one may write $\bar{\mathbf{k}}_{0,1} \equiv \bar{\mathbf{k}} = (\cos \alpha, \sin \alpha, 0)$, where the angle α as current angle between $\bar{\mathbf{k}}$ and $\bar{\mathbf{e}}_1 \parallel [100]$. The vector $\bar{\mathbf{k}}$ and axis $[001]$ give us an orthogonal basis to explain the vector $\bar{\mathbf{d}}$. Consequently, one can easily obtain that $\bar{\mathbf{d}} = (-\sin \alpha \cdot \sin \beta, \cos \alpha \cdot \sin \beta, \cos \beta)$, where β is the angle between $\bar{\mathbf{d}}$ and $\bar{\mathbf{e}}_3 \parallel [001]$, so that $\bar{\mathbf{d}} \parallel [001]$ when $\beta = 0$. As a result, one yields

$$\mathbf{p}_{\text{eff}} = \mathbf{p}_{13} \sin^2 \beta + \mathbf{p}_{33} \cos^2 \beta. \quad (2.11)$$

This formula can be simulated numerically with $\mathbf{p}_{13} = 0.340$ and $\mathbf{p}_{33} = 0.240$ for a TeO_2 -crystal [2.5, 2.6], see Fig.2.3.

The oscillating plot exhibits a minimum magnitude with $\mathbf{p}_{\text{eff min}} = 0.24$ at $\beta = \pi k$ and a maximum magnitude $\mathbf{p}_{\text{eff max}} = 0.34$ at $\beta = (\pi/2) + \pi k$. The magnitude inherent in the figure of acousto-optical merit is related to the normal regime of light scattering in a TeO_2 single crystal and equals to $\mathbf{M}_2 = \mathbf{n}^6 (\mathbf{p}_{\text{eff}})^2 / (\rho \mathbf{V}^3)$. The availability of maxima for \mathbf{M}_2 depends radically on the magnitude of the refractive index as well.

Due to our case corresponds to $\bar{\mathbf{k}} \perp [001]$ in a uniaxial crystal, the eigen-states of light polarization are naturally associated with the refractive indices \mathbf{N}_E when $\bar{\mathbf{d}} \parallel [001]$ and $\beta = \pi k$ as well as with \mathbf{N}_O when $\bar{\mathbf{d}} \perp [001]$ and $\beta = (\pi/2) + \pi k$. Because $\mathbf{N}_O < \mathbf{N}_E$ in a TeO_2 single crystal, the problem needs additional estimations of maxima for \mathbf{M}_2 .

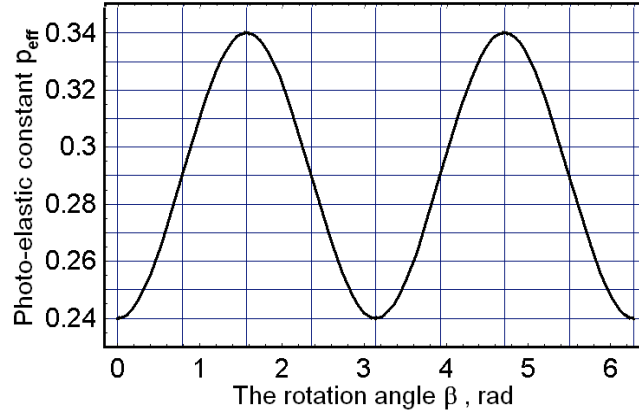


Figure 2.3. Dependence for the effective photo-elastic constant in a TeO_2 -single crystal versus the polarization rotation angle β inherent in the normal light scattering.

For instance, at the light wavelength $\lambda = 633$ nm, for example, this crystal has $N_E = 2.41$ and $N_O = 2.26$, so that, using the above-obtained data for p_{eff} , one can find $M_2 = 25.4 \cdot 10^{-18} \text{ s}^3/\text{g}$ for $\beta = \pi k$ (extraordinary light beams), and $M_2 = 34.6 \cdot 10^{-18} \text{ s}^3/\text{g}$ for $\beta = (\pi/2) + \pi k$, i.e. for ordinary light beams whose polarization is orthogonal to the optical axis of this crystal. The performed calculations demonstrate that the normal regime of scattering the ordinary polarized light by the longitudinal elastic wave is rather efficient in a TeO_2 -single crystal.

2.4. EFFICIENCY OF LIGHT SCATTERING IN A GALLIUM PHOSPHIDE SINGLE CRYSTAL

A gallium phosphide (GaP) single crystal has a cubic symmetry (point symmetry group is $\bar{4}3m$) and the transparency range $0.6\text{--}10 \mu\text{m}$. Then, $\rho_0 = 4.13 \text{ g/cm}^3$ is the material density of a GaP crystal, p_{eff} is the effective photo-elastic constants for light scattering, respectively; the refractive index is, for example, $n = 3.31$ at $\lambda = 671$ nm. In the case of a GaP -crystal, whose point symmetry group is $\bar{4}3m$, one can write [2.4] in the standard crystallographic axes. Then, let us assume that the longitudinal acoustic wave is passing along the $[110]$ -axis in a GaP -crystal whose vector of displacement is oriented along the same $[110]$ -axis. By this it means that $\vec{m} = \vec{u} = 2^{-1/2}(1, 1, 0)$.

$$p_{\lambda\mu} = \begin{pmatrix} p_{11} & p_{12} & p_{12} & 0 & 0 & 0 \\ p_{12} & p_{11} & p_{12} & 0 & 0 & 0 \\ p_{12} & p_{12} & p_{11} & 0 & 0 & 0 \\ 0 & 0 & 0 & p_{44} & 0 & 0 \\ 0 & 0 & 0 & 0 & p_{44} & 0 \\ 0 & 0 & 0 & 0 & 0 & p_{44} \end{pmatrix} \quad (2.12)$$

The corresponding normalized tensor of deformations is given by $\hat{\gamma} = (1/2)(\vec{e}_1 \cdot \vec{e}_1 + \vec{e}_2 \cdot \vec{e}_2 + \vec{e}_1 \cdot \vec{e}_2 + \vec{e}_2 \cdot \vec{e}_1)$ or in matrix notations by $\gamma_\mu = (1/2)(1, 1, 0, 0, 0, 1)$.

Performing the matrix multiplication and converting the product $\mathbf{p}_{\lambda\mu} \gamma_{\mu}$ to the conventional indices, one can obtain the admixtures ζ_{ij} to the dielectric impermeability tensor $\hat{\kappa}$ in the form

$$\hat{\zeta} = \hat{\mathbf{p}} \hat{\boldsymbol{\gamma}} = \frac{1}{2} \begin{pmatrix} \mathbf{p}_{11} + \mathbf{p}_{12} & 2\mathbf{p}_{44} & \mathbf{0} \\ 2\mathbf{p}_{44} & \mathbf{p}_{11} + \mathbf{p}_{12} & \mathbf{0} \\ \mathbf{0} & \mathbf{0} & 2\mathbf{p}_{12} \end{pmatrix} = \frac{1}{2} (\mathbf{p}_{11} + \mathbf{p}_{12}) (\bar{\mathbf{e}}_1 \cdot \bar{\mathbf{e}}_1 + \bar{\mathbf{e}}_2 \cdot \bar{\mathbf{e}}_2) + \mathbf{p}_{12} (\bar{\mathbf{e}}_3 \cdot \bar{\mathbf{e}}_3) + \mathbf{p}_{44} (\bar{\mathbf{e}}_1 \cdot \bar{\mathbf{e}}_2 + \bar{\mathbf{e}}_2 \cdot \bar{\mathbf{e}}_1). \quad (2.13)$$

The matrix of admixtures $\hat{\zeta}$ is a non-diagonal one, and both normal and anomalous light scattering can be potentially expected. Using Eq.(2.13), the effective photo-elastic constant can be expressed as

$$\mathbf{p}_{\text{eff}} = \bar{\mathbf{d}}^{(s)} \hat{\zeta} \bar{\mathbf{d}}^{(i)} = \frac{1}{2} \bar{\mathbf{d}}^{(s)} \begin{pmatrix} \mathbf{p}_{11} + \mathbf{p}_{12} & 2\mathbf{p}_{44} & \mathbf{0} \\ 2\mathbf{p}_{44} & \mathbf{p}_{11} + \mathbf{p}_{12} & \mathbf{0} \\ \mathbf{0} & \mathbf{0} & 2\mathbf{p}_{12} \end{pmatrix} \bar{\mathbf{d}}^{(i)}. \quad (2.14)$$

Due to $\bar{\mathbf{K}} \parallel [110]$, it is obvious that if the Bragg angles are omitted as small values, the wave vectors $\bar{\mathbf{k}}_0$ and $\bar{\mathbf{k}}_1$ of the incident and scattered light beams, respectively, should lie in the (110) -plane to be orthogonal to $\bar{\mathbf{K}}$. Moreover, one can put $\bar{\mathbf{k}}_0 = \bar{\mathbf{k}}_1 = \bar{\mathbf{k}}$ when the Bragg angles are neglected, so that one may write $\bar{\mathbf{k}}_{0,1} \equiv \bar{\mathbf{k}} = (\mathbf{a}, \mathbf{b}, \cos \alpha)$, where the angle α as current angle between $\bar{\mathbf{k}}$ and $\bar{\mathbf{e}}_3 \parallel [001]$. Obviously $\bar{\mathbf{k}} \perp [110]$, so that $\bar{\mathbf{k}} \cdot 2^{-1/2} (1, 1, 0) = 0$, hence $\mathbf{b} = -\mathbf{a}$ and $\bar{\mathbf{k}} = (\mathbf{a}, -\mathbf{a}, \cos \alpha)$. Because of $|\bar{\mathbf{k}}| = 1$, one can find $\bar{\mathbf{k}} = (2^{-1/2} \sin \alpha, -2^{-1/2} \sin \alpha, \cos \alpha)$. Now, the vector $\bar{\mathbf{k}}$ and the axis $[110]$ give us an orthogonal basis to explain the light polarization vector $\bar{\mathbf{d}}$. Naturally, one can require $\bar{\mathbf{d}} = (\mathbf{d}_1, \mathbf{d}_2, \mathbf{d}_3) \perp \bar{\mathbf{k}}$, so that $\bar{\mathbf{d}} \cdot \bar{\mathbf{k}} = 0$, hence $\mathbf{d}_3 = 2^{-1/2} (\mathbf{d}_2 - \mathbf{d}_1) \tan \alpha$. Then, one can determine the angle β by the relation $\bar{\mathbf{d}} \cdot 2^{-1/2} (1, 1, 0) = \cos \beta$, so that $\bar{\mathbf{d}} \parallel [110]$ when $\beta = 0$. It leads to $\mathbf{d}_1 + \mathbf{d}_2 = 2^{1/2} \cos \beta$. Finally, because $|\bar{\mathbf{d}}| = 1$, one can find the components $\mathbf{d}_1 = 2^{-1/2} (\cos \beta \pm \cos \alpha \cdot \sin \beta)$, $\mathbf{d}_2 = 2^{-1/2} (\cos \beta \mp \cos \alpha \cdot \sin \beta)$, and $\mathbf{d}_3 = \mp \sin \alpha \cdot \sin \beta$. Using the substitution $\beta \Rightarrow \beta + \pi/2$, one can obtain the components of the other vector $\bar{\mathbf{g}} = (\mathbf{g}_1, \mathbf{g}_2, \mathbf{g}_3) \perp \bar{\mathbf{d}}$, describing the light polarization, with the components: $\mathbf{g}_1 = 2^{-1/2} (-\sin \beta \pm \cos \alpha \cdot \cos \beta)$, $\mathbf{g}_2 = 2^{-1/2} (-\sin \beta \mp \cos \alpha \cdot \cos \beta)$, and $\mathbf{g}_3 = \mp \sin \alpha \cdot \cos \beta$. In the case of normal light scattering, i.e. with $\bar{\mathbf{d}}^{(s)} = \bar{\mathbf{d}}^{(i)} = \bar{\mathbf{d}}$, Eq. (2.14) gives

$$\mathbf{p}_{\text{eff},n} = \bar{\mathbf{d}} \hat{\zeta} \bar{\mathbf{d}} = \mathbf{d}_1^2 (\mathbf{p}_{11} + \mathbf{p}_{12}) + 2\mathbf{d}_1 \mathbf{d}_2 \mathbf{p}_{44} + \mathbf{d}_3^2 \mathbf{p}_{12}. \quad (2.15)$$

Within the case of anomalous light scattering when, for example, $\bar{\mathbf{d}}^{(s)} = \bar{\mathbf{g}}$ and $\bar{\mathbf{d}}^{(i)} = \bar{\mathbf{d}}$, Eq. (2.14) leads to

$$\mathbf{p}_{\text{eff},an} = \bar{\mathbf{g}} \hat{\zeta} \bar{\mathbf{d}} = \frac{1}{2} (\mathbf{d}_1 \mathbf{g}_1 + \mathbf{d}_2 \mathbf{g}_2) (\mathbf{p}_{11} + \mathbf{p}_{12}) + (\mathbf{d}_1 \mathbf{g}_2 + \mathbf{d}_2 \mathbf{g}_1) \mathbf{p}_{44} + \mathbf{d}_3 \mathbf{g}_3 \mathbf{p}_{12}. \quad (2.16)$$

These formulas can be simulated numerically with $\mathbf{p}_{11} = -0.151$, $\mathbf{p}_{12} = -0.082$ and $\mathbf{p}_{44} = -0.074$ for GaP -crystal [2.5, 2.6], see Fig.2.4.

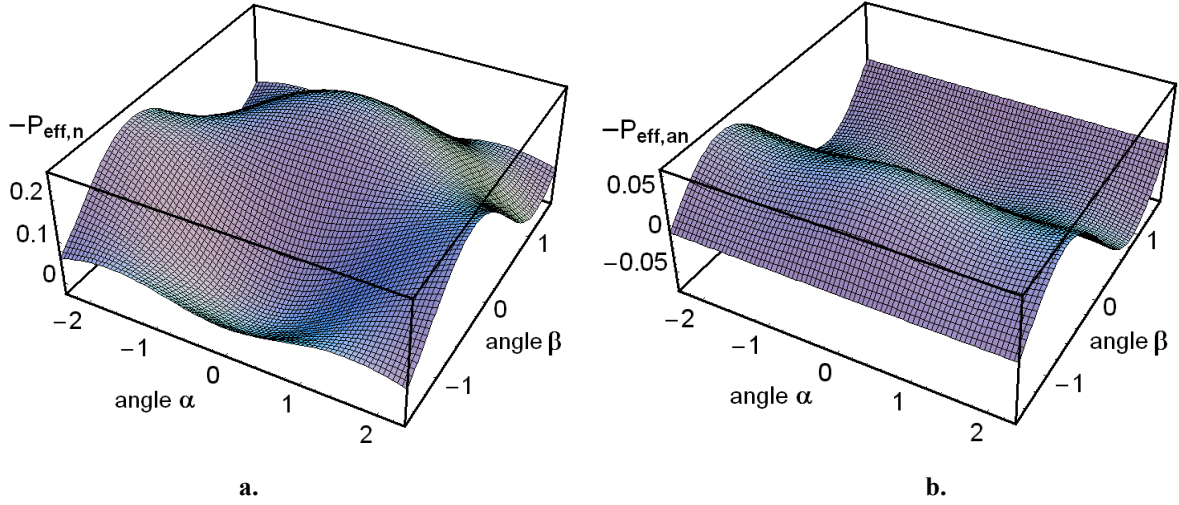


Figure 2.4. The effective photo-elastic constants in a **GaP** single crystal versus the angles α and β inherent in the normal (a) and anomalous (b) regimes of light scattering.

The oscillating plot exhibits a maximum magnitude of normal light scattering connected with the effective photo-elastic constant $|\mathbf{p}_{\text{eff},n}|_{\text{max}} = 0.1905$ at $\alpha = 0$ and $\beta = 0$. This value exceeds significantly the corresponding estimation for anomalous light scattering due to $|\mathbf{p}_{\text{eff},an}|_{\text{max}} \leq 0.05$ at any angles. The magnitude inherent in the figure of acousto-optical merit is related to the normal regime of light scattering in a **GaP** single crystal and equals to $\mathbf{M}_2 = \mathbf{n}^6 (\mathbf{p}_{\text{eff}})^2 / (\rho \mathbf{V}^3)$. For the above-taken longitudinal acoustic wave, passing along the $[\mathbf{110}]$ -axis in a **GaP** – crystal with the displacement vector oriented along the same $[\mathbf{110}]$ -axis, the acoustic wave velocity is $\mathbf{V} = 6.32 \cdot 10^5 \text{ cm/s}$. Consequently, one can estimate $\mathbf{M}_2 = 45.78 \cdot 10^{-18} \text{ s}^3/\text{g}$. The performed calculations demonstrate that the normal regime of light scattering by the longitudinal elastic wave is rather efficient in the chosen crystal. Finally, estimating the Klein-Cook parameter: $\mathbf{Q} = \mathbf{K}^2 \mathbf{L} / (\mathbf{n} \mathbf{k}) = 2 \pi \lambda \mathbf{L} \mathbf{f}^2 / (\mathbf{n} \mathbf{V}^2)$ with $\mathbf{n} = 3.31$, $\lambda = 671 \text{ nm}$, $\mathbf{L} = 0.1 \text{ cm}$, and $\mathbf{V} = 6.32 \cdot 10^5 \text{ cm/s}$, it is possible to find that one need at least $\mathbf{f} = 177 \text{ MHz}$ to obtain $\mathbf{Q} = 1$.

2.5. LINEAR ATTENUATION OF THE LONGITUDINAL ELASTIC WAVES AND ITS EFFECT ON THE EFFICIENCY OF LIGHT SCATTERING

Generally, the efficiency of acousto-optic interaction is affected by acoustic losses, which always exist in condensed matters. In the approximation of linear attenuation for the elastic waves, longitudinal or shear, the coefficient α of linear losses had been introduced. One of the most important parameters in the theory of acoustic attenuation represents the ratio of the acoustic wavelength Λ to the averaged mean free pass \mathbf{I}_F of thermal phonons in a crystal. Calling τ the averaged temporal interval between collision of thermal phonons and Ω the frequency of elastic wave, one can consider two limiting cases. If $\Lambda \ll \mathbf{I}_F$ and, consequently, $\Omega \tau \gg 1$, this is meant that the attenuation of acoustic phonons is conditioned by their collisions with a lattice whose phonons are in a state of thermal equilibrium. This case has been considered by L.Landau and G.Rumer [2.7], and G.L.Slonimsky [2.8]. Usually, it corresponds to the low temperature area, i.e. to the absolute temperature range of $< 50^\circ \text{ K}$, when the frequency of elastic wave is about 1 GHz . The opposite

case of $\Omega\tau \ll 1$ makes it possible to consider thermal phonons as particles propagating in a slowly varying potential field, caused by the acoustic wave. In fact, it means that the coherent elastic wave destroys an equilibrium distribution of thermal phonons, which become to be not governed by the equilibrium Planck distribution. Growing the entropy, needed for recovering the thermal equilibrium of these phonons, leads to attenuation of elastic energy. For the majority of crystals, this mechanism, revealed and described by A.Akhieser [2.9], can be observed at temperatures $> 50^0 \text{ K}$ and frequencies up to 1 GHz . The last case is very close to typical acousto-optic experimental situations. Evidently, the most compact and physically clear explanations related to this mechanism is done in Ref. [2.10], so that it is really worthwhile to apply just the Akhieser's mechanism to characterization of attenuating elastic waves in acousto-optical crystals. The above-mentioned coefficient α of linear losses can be introduced for both longitudinal and shear elastic waves more or less in the same manner. In these two cases the corresponding coefficients of linear losses have different values and slightly different determinations, but nevertheless they both exhibit the same frequency dependence in the range under consideration. This is why one can restrict him, for instance, by longitudinal elastic waves to explain all the needed peculiarities of affecting the light-scattering efficiency by acoustic losses.

For the longitudinal elastic waves one can use the following one-dimensional evolution scalar equation [2.11]

$$\frac{\partial^2 \mathbf{u}}{\partial x^2} - \frac{1}{V^2} \cdot \frac{\partial^2 \mathbf{u}}{\partial t^2} + \mathbf{b} \frac{\partial}{\partial t} \left(\frac{\partial^2 \mathbf{u}}{\partial x^2} \right) = \mathbf{0} \quad (2.17)$$

including the factor of acoustic losses \mathbf{b} . This factor is determined in Eq. (2.17) as $\mathbf{b} = \xi + \eta + \kappa (\mathbf{c}_V^{-1} - \mathbf{c}_P^{-1})$, where ξ and η represent coefficients for shear and bulk viscosities, κ is the coefficient for thermal conductivity, while \mathbf{c}_V and \mathbf{c}_P are specific heat capacities at constant volume and pressure, respectively. This equation can be applied to describing longitudinal elastic waves in isotropic media and in the particular cases of wave propagation along the acoustic axes in crystalline materials as well, so that the case of acoustic beam oriented along the $[001]$ -axis is perfectly acceptable for similar consideration. Potential solution to Eq. (2.17) can be taken in the form of $\mathbf{u}(\mathbf{x}, t) = \mathbf{A}(\mathbf{x}) \exp(-i\Omega t)$, leading to the following Helmholtz equation

$$\frac{d^2 \mathbf{A}}{dx^2} + \frac{\Omega^2}{V^2} (\mathbf{1} - i\mathbf{b}\Omega)^{-1} \mathbf{A} = \mathbf{0} \quad (2.18)$$

Substituting a standard trial function $\exp(i\chi x)$ in Eq. (2.18), one yields the quadratic algebraic characteristic equation $\chi^2 = \Omega^2 V^2 (\mathbf{1} - i\mathbf{b}\Omega)^{-1}$ whose solutions are given by

$$\begin{aligned} \text{a) } \chi_{1,2} &= \Omega V^{-1} (\mathbf{1} - i\mathbf{b}\Omega)^{-1/2} \approx \Omega V^{-1} [\mathbf{1} + i(\mathbf{b}\Omega/2)] = \mathbf{K} + i\alpha, \\ \text{b) } \mathbf{K} &= \Omega/V, & \text{c) } \alpha &= \mathbf{b}\Omega^2/(2V) \end{aligned} \quad (2.19)$$

in supposition that $(\mathbf{b}\Omega/2) \ll 1$; here $\mathbf{K} = |\vec{\mathbf{K}}|$ is the modulus of the wave vector $\vec{\mathbf{K}}$ of the elastic wave. Thus, one can express $\mathbf{A}(\mathbf{x}) = \mathbf{A}_1 \exp(i\chi_1 x) + \mathbf{A}_2 \exp(-i\chi_2 x)$ and then find $\mathbf{u}(\mathbf{x}, t)$ as

$$\mathbf{u}(\mathbf{x}, t) = \mathbf{A}_1 \exp(-\alpha x) \exp[-i\Omega(t - x/V)] + \mathbf{A}_2 \exp(\alpha x) \exp[-i\Omega(t + x/V)]. \quad (2.20)$$

This solution includes the two counter-propagating waves; each of them attenuates exponentially during its passing through a medium along the **[001]**– axis in opposite directions, so that for the positive direction of the axis \bar{x} one can choose only

$$\mathbf{u}(\mathbf{x}, t) = \mathbf{A}_1 \exp(-\alpha x) \exp[-i\Omega(t - x/V)]. \quad (2.21)$$

It is seen from Eq. (2.19c) that the factor α has a square-law dependence on the carrier frequency Ω of elastic wave in agreement with the Akhieser mechanism. This result is meant that amplitude of the longitudinal elastic wave decreases as $\exp(-\alpha x)$, while the energy transferring by this wave and the corresponding power vary as $\exp(-2\alpha x)$. To normalize the frequency dependence the acousto-optical materials are usually characterized by the constant $\Gamma = (\alpha/f^2) \text{ dB}/(\text{cm} \cdot \text{GHz}^2)$, where $f = \Omega/(2\pi)$ is the frequency of the chosen coherent elastic mode, so that, for example, if one takes the longitudinal elastic wave in a tellurium dioxide single crystal oriented along **[001]**– axis, the corresponding acoustic attenuation will be characterized by a factor of $\Gamma = 10 \text{ dB}/(\text{cm} \cdot \text{GHz}^2)$ [2.5, 2.6].

Now, one can consider the effect of acoustic attenuation along an aperture of acousto-optical cell within its operation in the Bragg regime of light scattering. The Bragg regime of light scattering in a lossless medium had been characterized above by the equations in Section 2.1. Taking into account the attenuation of total energy in a volume of a deformed body, one can find both the acoustic power density and the modulation parameter \mathbf{q} as

$$\text{a) } \mathbf{P} = \frac{1}{2} \rho V^3 \mathbf{u}^2 \exp(-2\alpha x), \quad \text{b) } \mathbf{q} \cong \pi \mathbf{u} \exp(-\alpha x) \cdot (2\lambda \cos \theta_B)^{-1} \sqrt{\rho V^3 M_2}. \quad (2.22)$$

Usually, during the spectrum analysis the partial magnitude of the parameter \mathbf{q} for each individual spectral component of a radio-signal is really small, so that one can approximate $\mathbf{I}_1 = \sin^2(\mathbf{qz}) \approx (\mathbf{qz})^2$ in the acousto-optical cell with linear acoustic losses. For the regime of a one-phonon light scattering, such an approximation can be successfully done in a vicinity of the point $\mathbf{qz} = \mathbf{0}$. In this case, the real-valued amplitude $\mathbf{E}_1(\mathbf{x}, \mathbf{z})$ of light field scattered into the first order, i.e. the issuing light amplitude at the output facet of acousto-optical cell, is directly proportional to the modulation parameter \mathbf{q} , so that one can obtain

$$\text{a) } \mathbf{E}_1(\mathbf{x}, \mathbf{z}) = \mathbf{E}_1(\mathbf{z}) \mathbf{E}_1(\mathbf{x}), \quad \text{b) } \mathbf{E}_1(\mathbf{x}) = \exp(-\alpha x), \quad \text{c) } \mathbf{E}_1(\mathbf{z}) \approx \mathbf{qz} = \frac{\pi z \mathbf{U}}{2\lambda \cos \theta_B} \sqrt{\rho V^3 M_2}. \quad (2.23)$$

If \mathbf{D} is the physical optical aperture of a cell measured in centimeters, one can introduce the normalized dimensionless coordinate $y = x/\mathbf{D}$ along the aperture with $y \in [0, 1]$ as well as the dimensionless amplitude parameter $\alpha_0 = \alpha \mathbf{D}$ for the acoustic losses along that optical aperture, so that $\alpha x = \alpha_0 y$; herein $\alpha [\text{cm}^{-1}] = 0.115 \cdot \alpha [\text{dB}/\text{cm}]$ for the amplitude parameter. Equation (2.23b) shows that the utilization for the incident light intensity can be characterized by the distribution of acoustic power along the optical aperture of a cell. Thus a relative portion of the optical power scattered by the attenuating acoustic beam can be characterized by

$$\mathbf{I}_A = \int_0^1 \exp(-2\alpha_0 y) dy = \frac{1 - \exp(-2\alpha_0)}{2\alpha_0}. \quad (2.24)$$

The corresponding plots, expressed as the function of amplitude parameter of total acoustic losses along c the cell's optical aperture in relative units and in decibels, are presented in Fig.2.5.

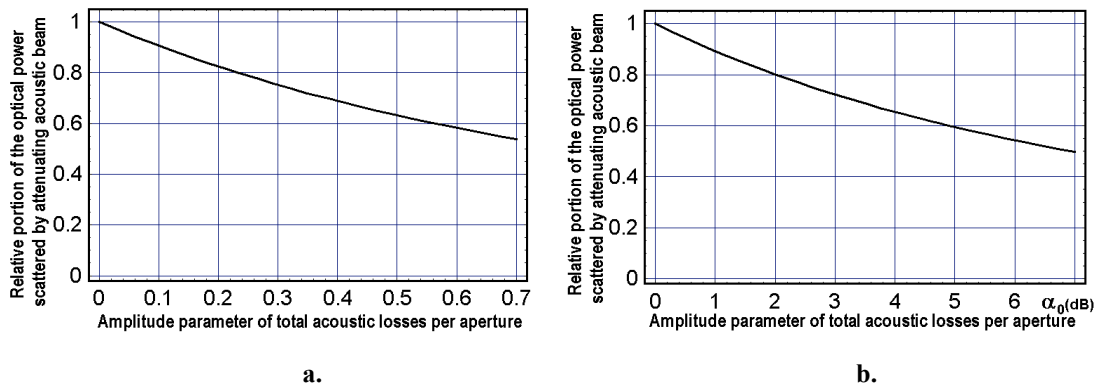


Figure 2.5. Relative portion of the scattered of optical power versus the amplitude parameter of total acoustic losses along the cell's optical aperture in relative units (a) and in decibels (b).

3. Estimating the time – bandwidth product of acousto-optical cells operating in the normal light scattering regime in some crystals

The TBWP is one of the important parameters peculiar to an acousto-optical cell in signal processing. It characterizes either the degree of complexity inherent in admissible signal or performance data of optical system. The frequency bandwidth of a cell depends on the chosen regime of acousto-optical interaction light scattering. Assuming that $\cos \theta_0 \approx 1$ in the simplest case of just normal regime of a one-fold light scattering, the frequency bandwidth can be obtained in the form

$$\Delta f_N = \frac{2nV^2}{\lambda L f_C} . \quad (3.1)$$

Here, n is an averaged refractive index of a crystalline material, f_C is the central acoustic frequency. Then, the frequency resolution of acousto-optical cell is determined by the formula $\delta f \approx V/D$. However, the time of passing the acoustic wave through a cell (or the time delay) can be estimated as $T = 1/\delta f \approx D/V$. Thus, the TBWP is given by

$$T \cdot \Delta f_N = \frac{2nVD}{\lambda L f_C} = N , \quad (3.2)$$

where N is the number of resolvable spots. There are a few factors limiting the number of resolvable spots as a function of the frequency [3.1] The first of them is just Eq.(3.2), where one can assume $\Delta f \approx f_C/2$ with the aperture D as an additional free parameter:

$$N_1 \leq \frac{D}{V} \cdot \Delta f = \frac{D f_C}{2V} . \quad (3.3)$$

The acoustic beam divergence, as it is passing through the light beam, conditions the second geometrical limitation of the number N of resolvable spots. The condition, bounding the piezoelectric transducer length (or what is the same the initial length of acousto-optical interaction) L with the distance to the point of half power level in the near-field zone of acoustic wave, being practically equivalent to D , is $D = L^2 f_C / (2V)$ [3.2]. Then, the Bragg regime of a one-phonon light scattering is provided when the well-known Klein-Cook parameter $Q = (2\pi/n) \cdot (\lambda L f_C^2 / V^2)$ exceeds 2π [3.3]. Therefore, one can estimate that $L = nQV^2 / (2\pi\lambda f_C^2)$ with the fixed magnitude of Q as the case requires choosing. Substituting two last expressions for D and L into Eq.(3.3), one yields

$$N_2 \leq \frac{n^2 Q^2 V^2}{16\pi^2 \lambda^2 f_C^2} . \quad (3.4)$$

The third limitation is connected with the acoustic attenuation. It can also be represented as function of the central acoustic frequency f_C . Let us use the factor Γ of acoustic attenuation expressed in $[\text{dB}/(\text{cm} \cdot \text{GHz}^2)]$. If the level of acoustic attenuation B [dB] per all the aperture is acceptable, the size of allowable aperture is equal to $D \leq B\Gamma^{-1} f_C^{-2}$. Substituting this formula into Eq.(3.3), one yields

$$N_3 \leq \frac{B}{2\Gamma v f_C} \quad (3.5)$$

Thus, the number N of resolvable elements (spots) or, what is the same, the TBWP is restricted by a triplet of the above-mentioned independent limitations. In the particular case of a one-phonon normal light scattering, one can take the following set of rather effective and available materials.

3.1. TIME-BANDWIDTH PRODUCT OF THE ACOUSTO-OPTICAL CELLS BASED ON LEAD MOLYBDATE (PbMoO_4) SINGLE CRYSTAL

The values inherent in this crystalline material, when the longitudinal elastic mode produces the acoustic beam along the $[001]$ axis of that crystal, are: $v = 3.63 \cdot 10^5 \text{ cm/s}$, $\lambda = 532 \text{ nm}$, $n = 2.3$, and $\Gamma = 15 \text{ dB}/(\text{cm} \cdot \text{GHz}^2)$. The numerical estimations have been realized for the apertures $D = 4, 5, 6, 7 \text{ cm}$; the attenuation factors along the full aperture $B = 4, 5, 6 \text{ dB/aperture}$, and the Klein-Cook parameters $Q = 2\pi$ and $Q = 3\pi$, see Fig.3.1. One can see that a lead molybdate acousto-optical cell with $D = 5 \text{ cm}$, $Q > 2\pi$, and $B < 5 \text{ dB/aperture}$ is capable to provide $N \approx 2000$ resolvable spots in a one-phonon optimized anomalous light scattering regime at a frequency f_C of about 220 MHz .

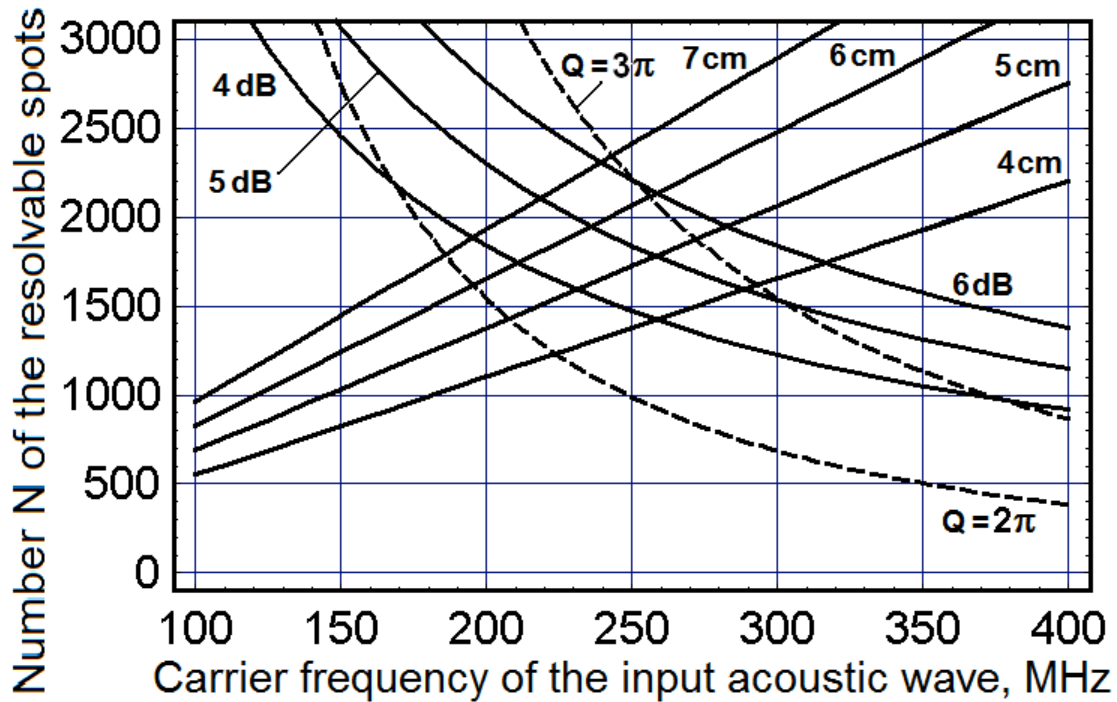


Figure 3.1. The combined diagram illustrating effect of a triplet of the restricting factors in a lead molybdate cell. The solid slowly growing lines are related to N_1 , the chosen apertures D are equal to 4, 5, 6, and 7 cm. The dashed line regards to N_2 in the cases of $Q = 2\pi$, and $Q = 3\pi$. The solid hyperbolic-like falling curves illustrate N_3 and reflect contributions of the acoustic attenuation; the attenuation factors B are equal to 4, 5, and 6 dB along the aperture.

3.2. TIME-BANDWIDTH PRODUCT OF THE ACOUSTO-OPTICAL CELLS USING A TELLURIUM DIOXIDE CRYSTAL (TeO_2) SINGLE CRYSTAL EXITED BY THE LONGITUDINAL ACOUSTIC MODE PASSING ALONG THE [001]- AXIS

Within a one-phonon light scattering in tellurium dioxide crystal, one can choose the normal process of acousto-optical interaction when the longitudinal elastic mode produces the acoustic beam along the [001] axis of that crystal. In this case, which competes with previously estimated case based on exploiting a lead-molybdate crystal based AOC, the following values: $V = 4.2 \cdot 10^5 \text{ cm/s}$, $\lambda = 633 \text{ nm}$, $n = 2.26$, and $\Gamma = 10 \text{ dB}/(\text{cm} \cdot \text{GHz}^2)$ are inherent in a TeO_2 crystal. The needed numerical estimations have been done for the optical apertures $D = 4, 5, 6, 7 \text{ cm}$; the attenuation factors along the full aperture $B = 4, 5, 6 \text{ dB/aperture}$, and the Klein-Cook parameter $Q = 3\pi, 4\pi$. One can see in Fig.3.2 that, for instance, a tellurium dioxide AOC with $D = 4 \text{ cm}$, $Q > 3\pi$, and $B = 4 \text{ dB/aperture}$ is capable to provide $N \approx 1500$ resolvable spots at $f_C \approx 320 \text{ MHz}$, while with $D = 5 \text{ cm}$, $Q > 4\pi$, and $B = 6 \text{ dB/aperture}$ the same cell is capable to provide $N \approx 2000$ resolvable spots at $f_C \approx 350 \text{ MHz}$.

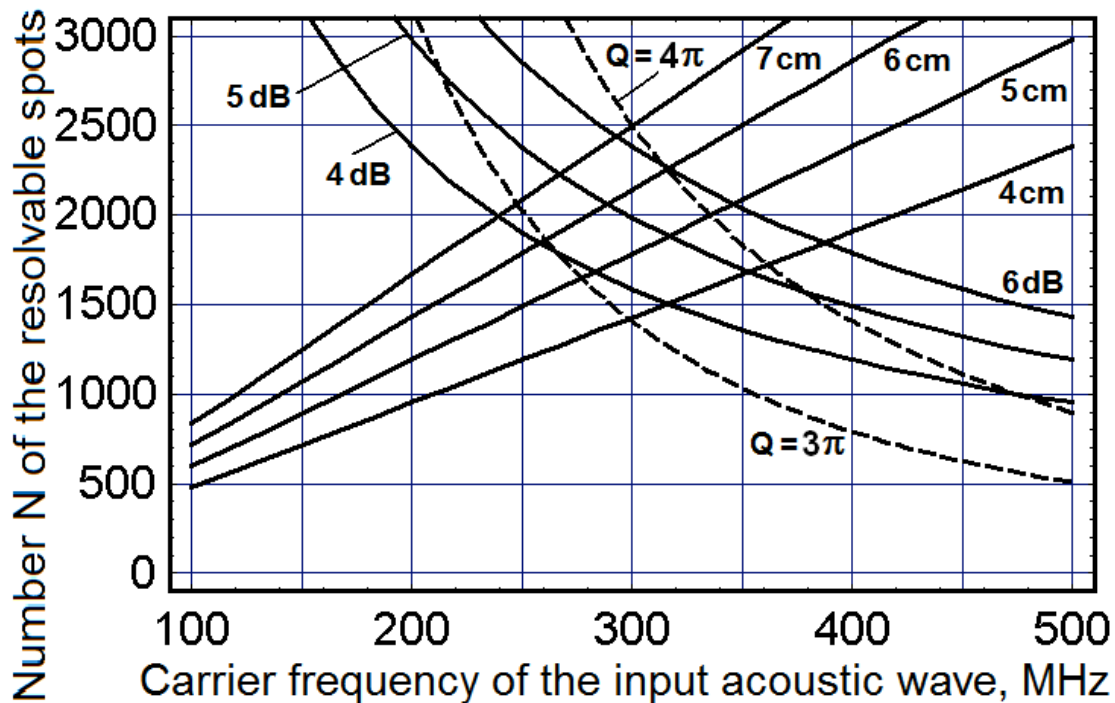


Figure 3.2. The combined diagram illustrating effect of a triplet of the restricting factors in a tellurium dioxide cell. The solid slowly growing lines are related to N_1 , the chosen apertures D are equal to 4, 5, 6, and 7 cm. The dashed line regards to N_2 in the case of $Q = 3\pi$ and 4π . The solid hyperbolic-like falling curves illustrate N_3 and reflect contributions of the acoustic attenuation; the attenuation factors B are equal to 4, 5, and 6 dB along the aperture.

3.3. TIME-BANDWIDTH PRODUCT OF THE ACOUSTO-OPTICAL CELLS BASED ON GALLIUM PHOSPHIDE (GaP) SINGLE CRYSTAL

The case of GaP -crystal is connected with the normal process when the longitudinal elastic mode produces the acoustic beam along the [110] axis, so that the following values inherent in this crystalline material: $V = 6.32 \cdot 10^5$ cm/s, $\lambda = 671$ nm, $n = 3.31$, and $\Gamma = 6$ dB/(cm · GHz²). The needed numerical estimations have been found for the apertures $D = 3, 4, 5, 6, 7$ cm; the attenuation factors along the full aperture $B = 4, 5, 6$ dB/aperture, and the Klein-Cook parameter $Q = 3\pi, 4\pi$, see Fig.3.3. One can see that, for example, a gallium phosphide acousto-optical cell with $D = 5$ cm, $Q \cong 2\pi$, and $B \approx 4.5$ dB/aperture is capable to provide $N \approx 1500$ resolvable spots at $f_C \approx 400$ MHz, while with $D = 7$ cm, $Q \cong 2\pi$, and $B \approx 5.5$ dB/aperture is capable to provide $N \approx 2000$ resolvable spots at $f_C \approx 350$ MHz,

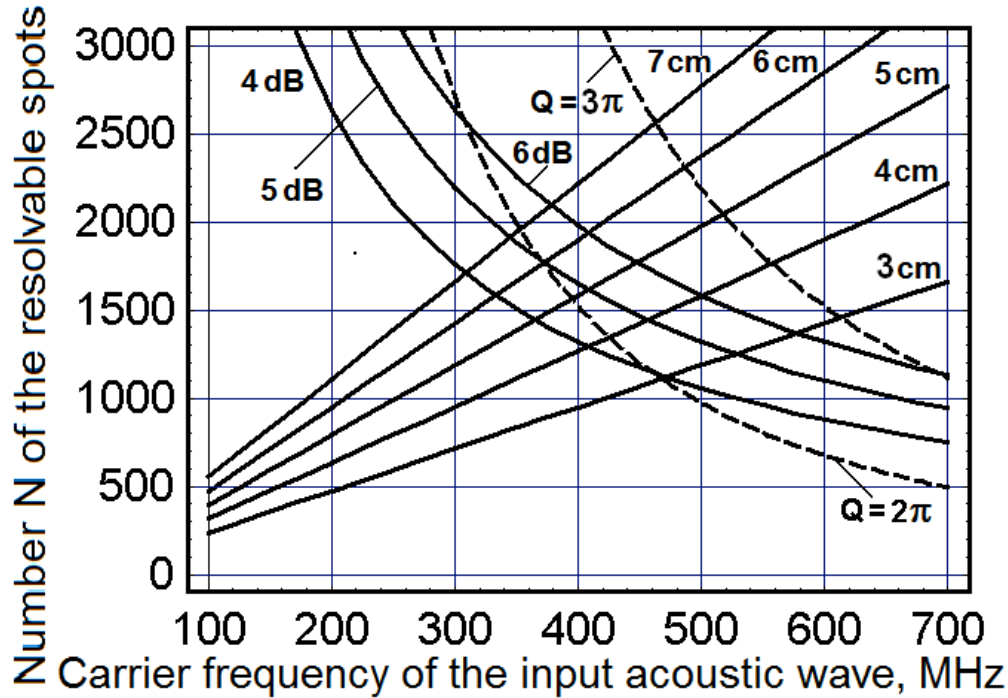


Figure 3.3. The combined diagram illustrating effect of a triplet of the restricting factors in a gallium phosphide cell. The solid slowly growing lines are related to N_1 , the chosen apertures D are equal to 3, 4, 5, 6, and 7 cm. The dashed line regards to N_2 in the case of $Q = 2\pi$ and 3π . The solid hyperbolic-like falling curves illustrate N_3 and reflect contributions of the acoustic attenuation; the attenuation factors B are equal to 4, 5, and 6 dB along the aperture.

These estimations for a triplet of the most effective and widely used crystalline materials have demonstrated that in each individual case the number N of resolvable spots, which is equivalent to the TBWP, does not exceed the values about 1500 – 2000. With some reasonable restrictions, one can consider these magnitudes as the natural limitation conditioned by various peculiarities of physical processes inherent in the normal regime of light scattering.

4. Time-bandwidth product of the acousto-optical cells based on the non-degenerated anomalous light scattering in TeO2 crystal

4.1. NON-DEGENERATED ANOMALOUS BRAGG LIGHT SCATTERING IN A CRYSTALLINE MATERIAL

Within normal Bragg interaction, an exact Bragg matching occurs at one frequency. Available frequency bandwidth is achieved by momentum-matching the distribution of acoustic plane waves generated by the finite-length piezoelectric transducer. Wider bandwidth is achieved by reducing the length of that transducer to create a larger distribution of acoustic wave vectors. The utility of this design technique is limited because the efficiency of the deflector is proportional to the piezoelectric transducer length. Within anomalous light scattering in a birefringent medium, an acoustic mode is used, which couples an extraordinary optical mode to an ordinary optical mode. For this technique Bragg matching over a large frequency bandwidth is possible without resorting to unacceptable small transducer lengths and hence low efficiencies. The standard phase-space representation of anomalous Bragg interaction is shown in Fig.4.1a for a positive uniaxial crystal. The refractive index ellipsoid consists for two surfaces, i.e. for two independent and polarized orthogonally to one another optical plane-wave states are allowed in the birefringent material. One state, the ordinary wave, is characterized by a directionally invariant main refractive index n_o . The other state, extraordinary wave is characterized by a directionally variant refractive index n_e . In fact, the optical normal surface of uniaxial crystal consists of a pair of the surfaces. One of them is a sphere of radius $2\pi n_o/\lambda$, while another is an ellipsoid of revolution. Within the standard approach to the non-degenerated anomalous light scattering in an anisotropic medium, the acoustic wave vector \vec{K} is arranged to lie tangential to the optical normal surface of the birefringent crystal. Hence, this interaction geometry is often referred to “tangential phase matching”. With this scheme, the Bragg matching occurs over a larger frequency range than that available from normal interaction in an isotropic medium where the acoustic wave vector \vec{K} bisects the optical normal surface. Additional frequency bandwidth is available by moving the acoustic wave vector parallel to itself away from the tangential condition [4.1], so that it lies on a line “optimal matching” constructed parallel to the tangent. Within this new arrangement with the same transducer plane, two acoustic wave vectors \vec{K}_1 and \vec{K}_2 intersect the optical normal surface, as it is shown in Fig.4.1b.

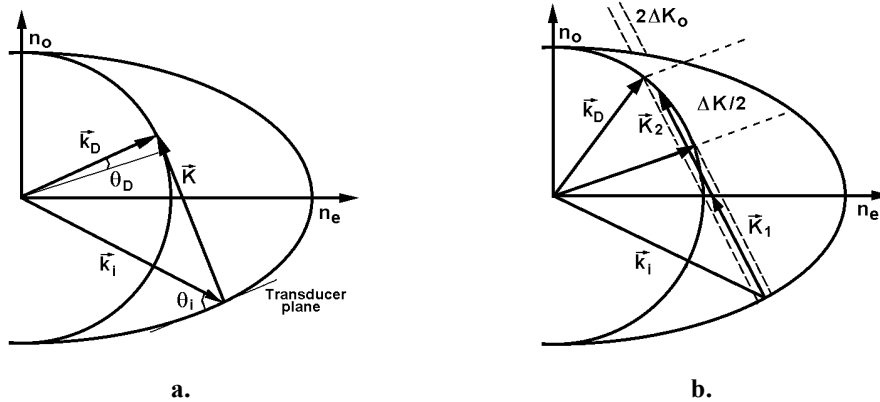


Figure 4.1. Vector diagram for a non-degenerated anomalous light scattering: the standard (a) and a wide bandwidth (b) arrangements, Ref.[4.1].

Hence, exact Bragg matching is achieved at two frequencies instead of one. This fact results in a symmetric bandshape, peaked at frequencies nominally equidistant from the center tangential matching frequency. To

achieve an equal-ripple bandshape over a bandwidth Δf_A , the optimal matching line is placed a distance ΔK_O away from the tangential line, so that it bisects the angular divergence of acoustic wave vectors $2\Delta K_O$. Using geometrical arguments, the range of acoustic wave vectors within the frequency bandwidth Δf_A of the deflector $\Delta K = 2\pi\Delta f_A/V$ can be written as

$$\frac{\Delta K}{2} = \sqrt{k_D^2 - (k_D - 2\Delta K_O)^2} \approx \sqrt{4k_D\Delta K_O}. \quad (4.1)$$

Here, the term ΔK_O^2 is omitted, as it is about three orders of magnitude smaller than k_D . The relation between an intermediate length K of the acoustic wave vector and the full angle of acoustic beam divergence $\varphi \approx \Lambda/L$ is $2\Delta K_O \approx K \cdot \varphi$, when $\tan \varphi \approx \varphi$. Using the above-noted expression for ΔK and the usual formula $k_D = 2\pi n_D/\lambda$, one can find from Eq.(4.1) that

$$L_O = \frac{8n_D V^2}{\lambda (\Delta f_A)^2}, \quad (4.2)$$

where the frequency bandwidth Δf_A is still not determined. Together with this, Eq.(3.1) gives $L \approx 2n_D V^2 / [\lambda (\Delta f_N) f_C]$. Comparing this expression with Eq.(4.2) with $\Delta f_A = \Delta f_N$, one can obtain the ratio $L_O/L \approx 4f_C/(\Delta f_N)$. For example, in widely used particular case of $\Delta f_N/f_C \approx 1/2$, the piezoelectric transducer can be about eight times longer. (This length, of course, is twice the length of the transducer required to achieve the same bandwidth when tangential matching condition is used). If visa verse $L_O = L$, one can find

$$(\Delta f_A)^2 = 4f_C \Delta f_N, \quad (4.3)$$

so that a significant bandwidth advantage is possible with the optimized anomalous light scattering in comparison with normal one under condition of $L_O = L$.

4.2. ESTIMATING THE TIME – BANDWIDTH PRODUCT OF ACOUSTO-OPTICAL CELL OPERATING IN THE NON-DEGENERATED ANOMALOUS LIGHT SCATTERING REGIME

From Eq.(4.1), one can express the frequency bandwidth Δf_A for anomalous light scattering as

$$\Delta f_A \approx 2V \sqrt{2n/(\lambda L)}, \quad (4.4)$$

where $L = L_O$ is the initial length of acousto-optical interaction. Then, Eq.(3.2) gives

$$N = T \cdot \Delta f_A \leq \frac{D}{V} \cdot \Delta f_A = 2D \cdot \sqrt{2n/(\lambda L)} \equiv N_1. \quad (4.5)$$

The frequency dependence is absent, but now one has the contribution of the piezoelectric transducer length L . Let us estimate the anomalous light scattering bandwidth using the above-noted approximation for the normal light scattering bandwidth by $\Delta f_N/f_C \approx 1/2$. One can find from Eq.(4.3) that

$$\text{a) } \Delta f_A = \sqrt{4f_C \Delta f_N} \approx f_C \sqrt{2}, \quad \text{b) } f_C \approx \Delta f_A / \sqrt{2} = 2V \sqrt{n/(\lambda L)}. \quad (4.6)$$

Equation (4.6b) makes it possible to determine the border frequencies f_{\min} and f_{\max} inherent in this bandwidth as

$$\begin{aligned} \text{a) } f_{\min} &= f_C - (\Delta f_A / 2) = f_C [1 - (\sqrt{2}/2)] \approx f_C (1 - 0.707) = 0.293 \cdot f_C, \\ \text{b) } f_{\max} &= f_C + (\Delta f_A / 2) = f_C [1 + (\sqrt{2}/2)] \approx f_C (1 + 0.707) = 1.707 \cdot f_C. \end{aligned} \quad (4.7)$$

Broadly speaking, estimations associated with these formulas can lead to appearing technical problem of matching the piezoelectric transducer with electronic circuits in rather wide frequency bandwidth exceeding an octave. This aspect can be illustrated by the following numerical example. Within a one-phonon light scattering in tellurium dioxide (TeO_2) crystal in the non-degenerated anomalous regime, one can choose the process exploiting the slow shear elastic mode along the $[110]$ axis of that crystal, so that in this case $V = 0.65 \cdot 10^5 \text{ cm/s}$, $\lambda = 633 \text{ nm}$, $n = 2.26$, and $L = 0.5 \text{ cm}$. Using Eqs.(4.6) and (4.7), one can calculate $\Delta f_A \approx 49.1 \text{ MHz}$ and $f_C \approx 34.74 \text{ MHz}$, which lead to $f_{\min} \approx 10.2 \text{ MHz}$ and $f_{\max} \approx 59.3 \text{ MHz}$. The obtained set of characteristic frequencies promises rather low contribution from acoustic attenuation, but exhibits the relative frequency width $f_{\max}/f_{\min} \approx 2.5$, i.e. close to 2.5 octaves. However, for the taken set of material parameters, estimating the Klein-Cook parameter at the frequency $f_{\min} \approx 10.2 \text{ MHz}$ gives $Q = (2\pi/n) \cdot (\lambda L f_{\min}^2 / V^2) \approx 2.167 < 2\pi$, which does not provide the Bragg regime of light scattering at f_{\min} . To avoid difficulties within a wide-band electronic matching and to increase the Klein-Cook parameter up to 2π or more the central carrier frequency has to be increased. Technically, such a step leads, in particular, to decreasing the relative frequency bandwidth and facilitates the process of wide-band electronic matching. This is why one has to increase the triplet of the characteristic frequencies f_C , f_{\min} , and f_{\max} up to F_C , F_{\min} , and F_{\max} , but to save the previously obtained frequency bandwidth Δf_A . Considering Klein-Cook parameter as a criterion, one can take a new minimal frequency $F_{\min}^{(0)} = 20 \text{ MHz}$, which leads to $Q \approx 8.33 > 2\pi$, i.e. exhibits almost the border minimal frequency. With such a new $F_{\min}^{(0)}$, one can find the following new values

$$\text{a) } F_C^{(0)} = F_{\min}^{(0)} + (\Delta f_A / 2) \approx 44.5 \text{ MHz}, \quad \text{b) } F_{\max}^{(0)} = F_{\min}^{(0)} + \Delta f_A \approx 69.1 \text{ MHz}. \quad (4.8)$$

Due to the bandwidth Δf_A is usually wide enough one has to use the new border values $F_{\min}^{(0)}$, and $F_{\max}^{(0)}$ to estimate the effects of acoustic beam divergence and acoustic attenuation. As before, the acoustic beam divergence, as it is passing through the light beam, conditions the second geometrical limitation for the number N of resolvable spots. Using all the previously formulated arguments, one can write the modified formulas, which are similar to Eqs.(3.4) and (3.5), expressed in terms of a new central frequency F_C , in particular of the border frequency $F_C^{(0)}$, and the bandwidth Δf_A as

$$N_2 \leq (\Delta f_A) \cdot \frac{n_0^2 Q^2 V^2}{8\pi^2 \lambda^2 [F_C - (\Delta f_A / 2)]^3} = \frac{n_0^2 Q^2 V^3}{4\pi^2 \lambda^2 [F_C - (\Delta f_A / 2)]^3} \cdot \sqrt{\frac{2n}{\lambda L}}, \quad (4.9)$$

$$N_3 \leq \frac{D}{V} \cdot (\Delta f_A) = \frac{B}{\Gamma V [F_C + (\Delta f_A / 2)]^2} \cdot \sqrt{\frac{2n}{\lambda L}}. \quad (4.10)$$

Thus, the number N of resolvable spots or, what is the same, a value of the TBWP is again restricted by a triplet of the above-mentioned independent limitations. Using the above-taken set of data for a TeO_2 -cell with $F_{\min}^{(0)} = 20 \text{ MHz}$ and $Q \approx 8.33$, one can find from Eqs.(4.5), (4.9), and (4.10) that

$$\begin{aligned} \text{a) } & \mathbf{B = 6 \text{ dB} , D = 5.25 \text{ cm} , N_1 \leq 3970 , N_2 \leq 29100 , \text{ and } N_3 \leq 6920 ;} \\ & \hspace{15em} (4.11) \\ \text{b) } & \mathbf{B = 8 \text{ dB} , D = 7.0 \text{ cm} , N_1 \leq 5300 , N_2 \leq 29100 , \text{ and } N_3 \leq 9230 .} \end{aligned}$$

One can see that now the Klein-Cook parameter Q provides the Bragg regime of light scattering at the frequency $F_{\min}^{(0)}$, while the relative frequency width $F_{\max}^{(0)}/F_{\min}^{(0)} \cong 1.5$ is much smaller, so that technical problem of matching the piezoelectric transducer with electronic circuits in rather wide frequency bandwidth does not appear. As a result, one can expect that the TBWP will be able to reach of about: (a) **4000** or (b) **5300**, as the case requires.

Nevertheless, from the viewpoint of increasing the dynamic range of a system the requirement for the Klein-Cook parameter Q can be raised, sometimes even at the cost of involving an increased acoustic attenuation. Let us slightly modify the previous example and take $L_1 = 0.3 \text{ cm}$, $D = 4.0 \text{ cm}$, and $B_1 = 10 \text{ dB}$. With this in mind, one can find $Q = (2\pi/n) \cdot [\lambda L_1 (F_{\min}^{(1)})^2 / V^2] \approx 18$ (more than 2 times higher than before), $F_{\min}^{(1)} = 38 \text{ MHz}$, $F_C^{(1)} = 70 \text{ MHz}$, $\Delta f_A^{(1)} \approx 64 \text{ MHz}$, and $F_{\max}^{(1)} = 102 \text{ MHz}$. Consequently, one yields: $N_1 \leq 3940$, $N_2 \leq 30640$, and $N_3 \leq 3940$. In this case the TBWP will be able to reach approximately a **4000**-level at the higher central frequency **70 MHz**.

4.3. EXPERIMENTAL DATA

Testing the optical system of an advanced prototype had been carried out with the Bragg cell, made of tellurium dioxide (TeO_2) crystal (Brimrose Corp.), which has an active optical aperture of about 40×2 mm. Within operating at the optical wavelength of **633** nm with linear state of the incident light polarization on the central acoustic frequency of about **75** MHz, this cell provides the deflection angle of about **3** angular degrees and allows a maximum input acoustic power of about **1.0** W. The acoustic wave velocity can be estimated by $V \approx 0.65 \cdot 10^5$ cm/s. The experimental studies consisted in two parts. The first one included measuring the bandwidths of acousto-optical interaction in the Bragg regime of light scattering in the first order. General schematic arrangement of the corresponding set-up for these measurements is presented in Fig.4.2.

The second part of our experiments was related to estimating possible resolution of the AOC under consideration. In fact, the intensity distributions of an individual spot in focal plane of the integrating lens for light scattering by a TeO_2 -cell in the first order had been measured. In so doing, the experimental set-up was arranged as it is shown in Fig.4.3. Figure 4.4 shows the experimental plot for the frequency response inherent in the TeO_2 -cell.

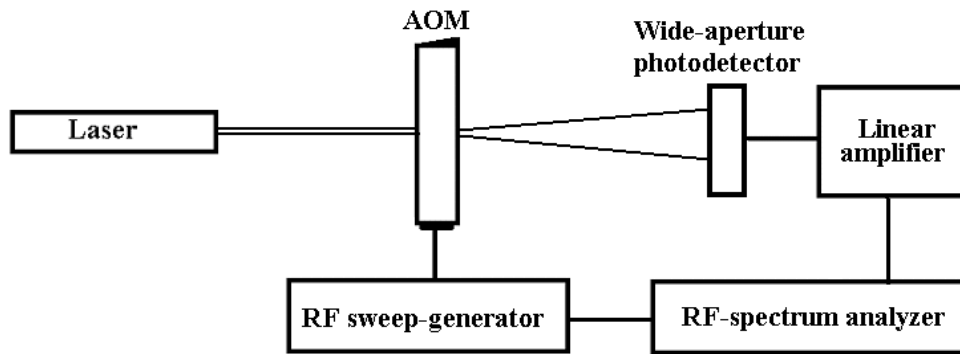


Figure 4.2. General schematic arrangement for measuring the frequency bandwidth of a TeO₂-cell.

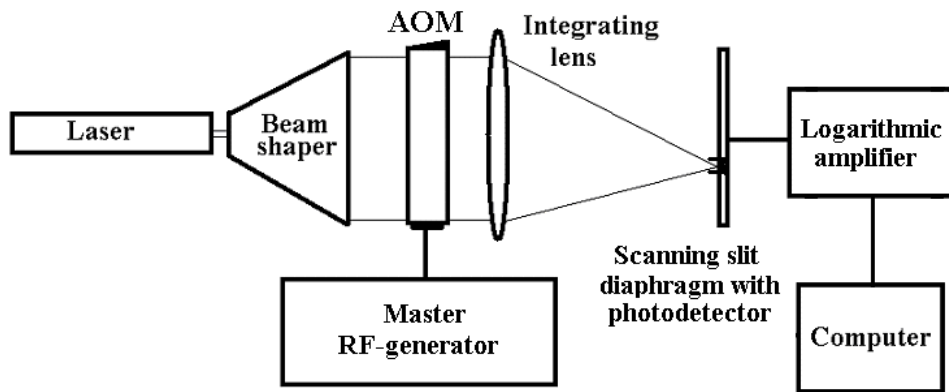
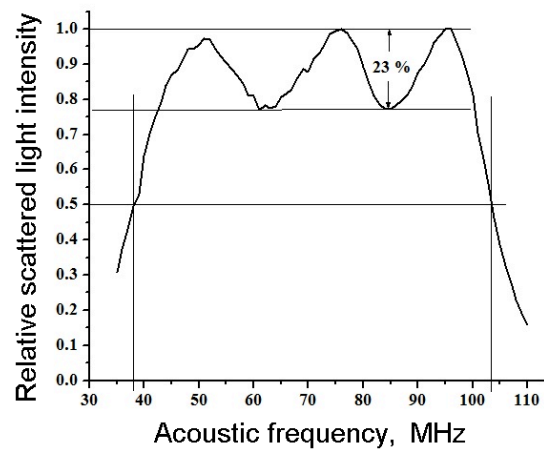


Figure 4.3. General schematic arrangement for measuring the intensity profile of an individual spot



a.



b.

Figure 4.4. A 40-mm aperture TeO₂-crystal based AO-cell from Brimrose Corp. (a) and the frequency response versus the input acoustic frequency applied at this AO-cell (b).

One can observe the characteristic variations of efficiency at a top of the experimental plot. This oscillation is motivated by some uncoupling of both active and reactive parts of the cell's impedance at different frequencies. Each maximum of efficiency is potentially corresponding to better matching of impedance at the takes radio-wave frequency. Practically obtained non-uniformity of the frequency characteristic is equal to about **23%** (i.e. less than **1.5 dB**). Total experimental frequency bandwidth at a **-3 dB**-level has been estimated by $\Delta f_{\text{exp}} \approx \mathbf{65.5}$ MHz.

5. Conclusive remarks

Then, the AOCs, exploiting lead molybdate crystals, so-called fast cut in tellurium-dioxide crystals, and gallium phosphide crystals, have been characterized and estimated from the points of views related to their acousto-optical parameters and the expected acoustic attenuation, which can potentially affect the shape of each individual resolvable spot at the output plane and, consequently, the dynamic range of processing. Moreover, the TBWP products of acousto-optical cells exploiting the normal light scattering in these materials have been characterized. From the above line of reasoning the AOC based on the specifically shifted cut of a tellurium dioxide single crystal has been considered as an optimal choice, and its TBWP has been analyzed theoretically and measured experimentally. In so doing, the model of estimating both the frequency bandwidth and the spectral resolution had been developed. The frequency bandwidth was precisely calculated including the contributions from terms in expansions related to optical anisotropy of this material as well as from really high acoustic anisotropy in the tellurium dioxide crystal leading to remarkable divergence for acoustic beams. The resolution was described using, in particular, corpuscular approach to this problem, which includes a look at the uncertainty principle. During the performed experiments, the tellurium dioxide AOC, produced with the specifically shifted crystalline cut providing the almost-shear acoustic wave velocity of $0.65 \cdot 10^5$ cm/s, with the clear optical aperture of **40 mm** operating within the radio-signal frequency range up to **100 MHz** had been used. As a result of the realized optimization, the frequency bandwidth of **65 MHz** had been achieved, so that experimental estimation for the obtained TBWP was equal to **4000**.

6. Acknowledgment

This work has been financially supported by the CONACyT, Mexico within the projects # 61237 (initially) and # 15149 (currently).

7. References

Chapter 1.

- [1.1] E. Young and S-K. Yao. "Design considerations for acousto-optic devices". Proc. IEEE, v.69, No. 1 p.54-64 (1981).

Chapter 2.

- [2.1] R. W. Klein and B. D. Cook. "A unified approach to ultrasonic light diffraction.", IEEE Transactions of Sonics and Ultrasonics, vol. **SU-14**, no. 3, pp. 123-134 (1967).
- [2.2] V. I. Balakshy, V. N. Parygin, and L. E. Chirkov. [Physical Principles of Acousto-Optics], Radio i Svyaz Press, Moscow, 1985.
- [2.3] E.I.Gordon. "A Review of Acoustooptical Deflection and Modulation Devices". Appl. Opt. v. **5**, no. 10, p.1629-1639 (1966).
- [2.4] Yu. I. Sirotin and M. P. Shaskolskaya. [Fundamentals of Crystal Physics], Mir Publishers. Moscow, 1982.
- [2.5] V. G. Dmitriev, G. G. Gurzadyan, and D. N. Nikogosyan. [Handbook of nonlinear optical crystals]. Springer-Verlag, New York, 1999.
- [2.6] A. A. Blistanov. [Crystals for Quantum and Nonlinear Optics], 2-nd. Ed., MISIS Publisher, Moscow, 2007.
- [2.7] L. D. Landau and G. Rumer. "Absorption of sound in solids." Phys. Zs. Sovjetunion. vol.**11**, pp.18-25 (1937).
- [2.8] G. A. Slonimsky. Soviet Physics: Journal of Experimental and Theoretical Physics. Vol.7, p.1457 (1937).
- [2.9] A. I. Akhieser. Soviet Physics: Journal of Experimental and Theoretical Physics. Vol.8, p.1318 (1938).
- [2.10] D. Ter Haar. [Elements of Statistical Mechanics]. Holt, Rinehart & Winston, New-York, 1954.

[2.11] M. B. Vinogradova, O. V. Rudenko, and A. P. Sukhorukov. [Theory of Waves], Nauka-Press. Moscow, 1990.

Chapter 3.

[3.1] E. Young and S-K.Yao. "Design considerations for acousto-optic devices". Proc. IEEE, v.69, No. 1 p.54-64 (1981).

[3.2] A.P. Goutzoulis and D. R. Pape. [Design and fabrication of acousto-optic devices], Chapter 2. Design of Acousto-Optic deflectors, Dennis R. Pape. p. 87

[3.3] R. W. Klein and B. D. Cook. "A unified approach to ultrasonic light diffraction.", IEEE Transactions of Sonics and Ultrasonics, vol. **SU-14**, no. 3, pp. 123-134 (1967).

Chapter 4.

[4.1] A.P. Goutzoulis and D. R. Pape. [Design and fabrication of acousto-optic devices], Chapter 2. Design of Acousto-Optic deflectors, Dennis R. Pape. p. 87.